

# Using Level Crossing Rate of Selection Combining Receiver Damaged by Beaulieu-Xie Fading and Rician Co-Channel Interference with a Purpose of Machine Learning QoS Level Prediction

Suad Suljovic<sup>1</sup>, Dragana S. Krstic<sup>2,\*</sup>, Goran Nestorovic<sup>1</sup>, Nenad N. Petrovic<sup>2</sup>, Sinisa Minic<sup>3</sup>, Devendra S. Gurjar<sup>4</sup>

<sup>1</sup>The Academy of Applied Technical Studies Belgrade,  
Katarine Ambrozic 3, 11000 Belgrade, Serbia

<sup>2</sup>Faculty of Electronic Engineering, University of Nis,  
A. Medvedeva 14, 18000 Nis, Serbia

<sup>3</sup>Faculty of Teacher Education in Prizren, University of Pristina in Kosovska Mitrovica,  
Nemanjina bb, 38218 Leposavic, Serbia

<sup>4</sup>Department of Electronics and Communications Engineering,  
National Institute of Technology Silchar,  
Assam, India

ssuljovic@atssb.edu.rs, \*dragana.krstic@elfak.ni.ac.rs, gnestorovic@atssb.edu.rs,  
nenad.petrovic@elfak.ni.ac.rs, sinisa.minic@pr.ac.rs, dsgurjar@ece.nits.ac.in

**Abstract**—In this paper, a wireless system is considered impacted by Beaulieu-Xie (BX) fading and Rician co-channel interference (CCI). A selection diversity combining technique is used to combat multi-path fading and CCI effects. The expression for the level crossing rate (LCR) is formulated for the receiver with more input branches, and the corresponding curves that have dependence on the signal-to-interference ratio (SIR) are drawn. On the basis of the presented graphs, we quantify the amount of LCR affected by the presence of fading and interference. Additionally, we propose a classification-based predictive model which leverages the previously calculated LCR value as one of inputs among other variables (number of users, base station, the day of the week) with the aim of Quality of Service (QoS) level prediction.

**Index Terms**—Beaulieu-Xie fading; Machine learning; Rician co-channel interference; Selection combining.

## I. INTRODUCTION

Since wireless communication systems are one of the fastest developing technologies in recent years, researchers in the field are looking for solutions to obtain higher data rates for new applications [1]. Moreover, the radio frequency band is overloaded, and new bands such as millimeter-wave (mmWave) and terahertz (THz) bands, femtocells, and wireless powered communication (WPC) systems are in the early stage of development. Fifth-generation (5G) cellular networks tend to the mmWave frequency spectrum to tolerate higher data transmission rates with low delays [2].

The biggest challenge is the need for correct channel modelling. Many measurements were made in different wireless environments to collect data on fading values. Measurements of small-scale fading at 28 GHz in outdoor mmWave ultra-wideband channels were made in [3]. After extensive measurements, the fluctuating two-rays (FTR) channel model is taken as a very suitable small-scale fading model for 5G mmWave wireless communication alongside known fading models [4]. Some other already well-known fading models are special cases of the FTR model: Rician, Rayleigh, Nakagami- $m$ , and also two waves with diffused power (TWDP) model.

After this point, the newly acquired Beaulieu-Xie (BX) distribution as a very well descriptive channel model was introduced into considerations [5]–[10]. The BX fading model has the property of characterising wireless systems with multiple line-of-sight (LOS) components that have arisen via direct propagation and specular reflections and non-line-of-sight (NLOS) components. The BX distribution model encompasses the Nakagami- $m$  distribution, which can control the number of clusters by variable  $m$ , and the Rician distribution that can simulate the environment when LOS, or deterministic component, is present in the received signal [11]. So, BX fading model is extremely useful since it combines the features of both Nakagami- $m$  and Rician fading models. Relations between the Nakagami- $m$ , Rician, Rayleigh, and BX distributions are presented in Fig. 1.3 in [5].

In addition to that, the BX distribution unites the next distributions with the help of which the wireless channels

are modelled: non-central chi, generalised Ricean, and  $\kappa$ - $\mu$  distributions. The relations between these distributions are presented in Table I in [6].

In [7], an analysis was done and the closed-form expression for effective capacity over BX fading based on delay constraints was derived. In [8], the closed-form expression for the average symbol error probability (ASEP) of generalised M-ary quadrature amplitude modulation (M-QAM) was derived over the BX fading channel. Furthermore, the probability of outage and error rate performance of maximal ratio combining, equal gain combining, and selection combining (SC) over arbitrarily correlated BX fading channels were considered in [9]. Here, different diversity combining schemes were used to mitigate fading influence. In [10], however, some first order system performance (outage probability, amount of fading, ASEP, and channel capacity) for coherent and non-coherent modulation schemes were derived for the Beaulieu-Xie fading channel.

All these papers considered a system without interference effects of signals. Subsequently, we present performance consideration of the BX fading channels in the presence of co-channel interference (CCI) for diversity receptions of the multi-branch SC technique utilised to improve system performance. We will deal with second-order system performance. Namely, we will derive the signal-to-interference ratio (SIR)-based level crossing rate (LCR) for such defined scenario.

Two important second-order statistics of multi-path fading channels are the LCR and the average fade duration (AFD). The LCR shows how often the envelope crosses a certain threshold required for communication, i.e., the LCR is average number of times per second that the envelope crosses the predefined level in the downward direction, while the AFD shows the average time the signal envelope spends below the threshold [1]. Knowledge of LCR and AFD helps with error correction and calculation of the average duration of outages of wireless communication systems [12].

Additionally, in the second part of the paper we integrate the proposed system model within network modelling and simulation environment and use the calculated value of the LCR utilising the graphics processing unit (GPU) for the purpose of predicting the quality of service (QoS) using machine learning. In that context, we treat the problem as classification and provide implementation using the Waikato Environment for Knowledge Analysis (Weka) framework in the Java programming language.

This paper consists of five sections. After the introduction, with reference to the first papers introducing BX fading in the literature, the model of observed scenario in our work is described in Section II. Section III presents the obtained results and gives a discussion of the system and the influence of parameters. Section IV determines QoS using Weka classification. The closing remarks and description of the future work are given in Section V.

## II. LEVEL CROSSING RATE OF SIGNAL-TO-INTERFERENCE RATIO AT THE OUTPUT OF THE RECEIVER

Multi-branch selection combining receiver in a Beaulieu-Xie fading channel additionally distracted by Rician co-

channel interference is a scenario for our investigation in this work. There are  $L$  input antennas in the SC receiver with copies of the useful signal marked by  $x_1, x_2, \dots, x_L$ . The corresponding output signal is  $x$ . The CCI signals appearing at the receiver input are denoted by  $y_1, y_2, \dots, y_L$ , while the corresponding output CCI is  $y$ . The ratio of the useful signal and the co-channel interference on the corresponding  $i^{\text{th}}$  branch at the SC receiver input is  $z_i = x_i/y_i$ .

In SC combining, the received signal from the antenna that experiences the highest SIR is passed to the user. Therefore, the output SIR (at the combiner output) is the maximum SIR of all received signals  $z_i$

$$z = \max(z_1, z_2, \dots, z_L). \quad (1)$$

The useful signals at the input of the receiver have the probability density function (PDF) modelled by the BX distribution ((4) in [6])

$$p_{x_i}(x_i) = \frac{2mx_i^m}{\Omega_i \lambda^{m-1}} e^{-\frac{m}{\Omega}(x_i^2 + \lambda^2)} I_{m-1}\left(\frac{2m\lambda}{\Omega_i} x\right). \quad (2)$$

In this PDF,  $m$  presents the fading severity parameter and controls the shape,  $\lambda$  presents the extension of distribution, i.e., the location and height of the mode of the PDF,  $\Omega_i$  reflects the power and controls the spread,  $\lambda^2$  represents the power of the LOS components, and furthermore,  $\lambda^2/\Omega$  is the Rician  $K$ -factor representing the ratio between the total average power of the components in LOS, and the total average power of the scattered components.

If modified Bessel function of the first kind and order  $\nu$   $I_\nu(\cdot)$  ((8.401) in [13]) from (2) is expressed by ((8.445) in [13])

$$I_\nu(x) = \sum_{k=0}^{\infty} \frac{(x/2)^{\nu+2k}}{k! \Gamma(\nu+k+1)}, \quad (3)$$

with Gamma function  $\Gamma(t)$ , the PDF of useful signal can be represented in the form

$$p_{x_i}(x_i) = 2e^{-\frac{m}{\Omega}(x_i^2 + \lambda^2)} \sum_{i_1=0}^{+\infty} \frac{\lambda^{2i_1} x_i^{2i_1+2m-1}}{i_1! \Gamma(i_1+m)} \left(\frac{m}{\Omega_i}\right)^{2i_1+m}. \quad (4)$$

The CCI envelope  $y_i$  is under Rician distribution [14]

$$p_{y_i}(y_i) = 2e^{-\frac{(1+K_i)y_i^2}{s_i} - K_i} \sum_{i_2=0}^{\infty} \frac{K_i^{i_2} y_i^{2i_2+1}}{i_2! \Gamma(i_2+1)} \left(\frac{1+K_i}{s_i}\right)^{i_2+1}. \quad (5)$$

In (5),  $s_i$  is the CCI power and  $K_i$  is the Rician factor equal to the ratio of direct and scattered components.

Now it is necessary to determine the PDF of SIR  $z_i$ . The formula for this PDF is [15]

$$p_{z_i}(z_i) = \int_0^{\infty} p_{x_i}(z_i y_i) p_{y_i}(y_i) dy_i. \quad (6)$$

By exchange of  $x_i = z_i \times y_i$ , and then putting formulas (4) and (5) in (6), we get

$$p_{z_i}(z_i) = 2e^{-\frac{m}{\Omega_i}\lambda^2 - K_i} \sum_{i_1=0}^{+\infty} \sum_{i_2=0}^{+\infty} \frac{K_i^{i_2}}{i_1! i_2!} \times \frac{\lambda^{2i_1} z_i^{2i_1+2m-1} m^{2i_1+m} s_i^{i_1+m} (1+K_i)^{i_2+1} \Gamma(i_1+i_2+m+1)}{\Gamma(i_1+m)\Gamma(i_2+1)\Omega_i^{i_1-i_2-1} (\Omega_i(1+K_i) + ms_i z_i^2)^{i_1+i_2+m+1}}. \quad (7)$$

Furthermore, we should derive the cumulative distribution function (CDF) of the SIR  $z_i$  from [1]

$$F_{z_i}(z_i) = \int_0^{z_i} p_{z_i}(t) dt. \quad (8)$$

Utilising formula (7) and introducing into (8) leads to the following formula for the CDF of the SIR  $z_i$  [16]

$$F_{z_i}(z_i) = 2e^{-\frac{m}{\Omega_i}\lambda^2} e^{-K_i} \times \sum_{i_1=0}^{+\infty} \sum_{i_2=0}^{+\infty} \frac{K_i^{i_2} m^{2i_1+m} (1+K_i)^{i_2+1}}{i_1! i_2! \Omega_i^{i_1-i_2-1}} \times \frac{\lambda^{2i_1} s_i^{i_1+m} \Gamma(i_1+i_2+m+1)}{\Gamma(i_1+m)\Gamma(i_2+1)} \times \int_0^{z_i} \frac{t^{2i_1+2m-1}}{(\Omega_i(1+K_i) + ms_i t^2)^{i_1+i_2+m+1}} dt. \quad (9)$$

To solve the integral in (9), we used (6) from [16] based on [12], where  $B_w(c, d)$  is the incomplete Beta function ((8.39) in [13]). With adequate replacement in (9), CDF becomes

$$F_{z_i}(z_i) = e^{-\frac{m}{\Omega_i}\lambda^2 - K_i} \sum_{i_1=0}^{+\infty} \sum_{i_2=0}^{+\infty} \frac{K_i^{i_2} \lambda^{2i_1}}{i_1! i_2!} \left(\frac{m}{\Omega_i}\right)^{i_1} \times \frac{\Gamma(i_1+i_2+m+1)}{\Gamma(i_1+m)\Gamma(i_2+1)} B_{\frac{ms_i z_i^2}{\Omega_i(1+K_i) + ms_i z_i^2}}(i_1+m, i_2+1). \quad (10)$$

We tend to obtain the LCR of a random process  $z_i$ . LCR is calculated as the mean value of the first derivative of the envelope of observed random process. The formula for LCR from [1] is

$$N_{z_i}(z_i) = \int_0^{\infty} \dot{z}_i p_{z_i z_i}(\dot{z}_i, z_i) d\dot{z}_i. \quad (11)$$

To solve (11), we should find the first derivative of SIR  $z_i$  defined as  $z_i = x_i/y_i$ . Namely, the first derivative for such a defined  $z_i$  is

$$\dot{z}_i = \frac{1}{y_i} \dot{x}_i - \frac{x_i}{y_i^2} \dot{y}_i. \quad (12)$$

Next, the mean value and variance of  $\dot{z}_i$  should be determined. The mean value of  $\dot{z}_i$  is

$$\bar{\dot{z}}_i = \frac{1}{y_i} \bar{\dot{x}}_i - \frac{x_i}{y_i^2} \bar{\dot{y}}_i = 0, \quad (13)$$

and the variance of  $\dot{z}_i$  is

$$\sigma_{\dot{z}_i}^2 = \frac{1}{y_i^2} \sigma_{\dot{x}_i}^2 + \frac{x_i^2}{y_i^4} \sigma_{\dot{y}_i}^2. \quad (14)$$

The variance of the useful signal  $x_i$  is ((2.4) in [6])

$$\sigma_{x_i}^2 = \frac{\pi^2 f_m^2 \Omega_i}{m} \quad (15)$$

and the variance of CCI  $y_i$  is

$$\sigma_{y_i}^2 = \frac{\pi^2 f_m^2 s_i}{(K_i + 1)}. \quad (16)$$

In (15) and (16),  $f_m$  denotes the Doppler frequency.

After substituting (15) and (16) in (14), the expression for variance of  $\dot{z}_i$  becomes

$$\sigma_{\dot{z}_i}^2 = \frac{\pi^2 f_m^2}{y_i^2 m (K_i + 1)} (\Omega_i (K_i + 1) + ms_i z_i^2). \quad (17)$$

The conditional PDFs of  $z_i$ ,  $\dot{z}_i$ , and  $y_i$  are [16]:

$$p_{\dot{z}_i}(\dot{z}_i | z_i, y_i) = \frac{1}{\sqrt{2\pi} \sigma_{\dot{z}_i}} e^{-\frac{\dot{z}_i^2}{2\sigma_{\dot{z}_i}^2}}, \quad (18)$$

$$p_{z_i}(z_i | y_i) = \left| \frac{dx_i}{dz_i} \right| p_{x_i}(z_i y_i) = y_i p_{x_i}(z_i y_i). \quad (19)$$

The conditional joint PDF (JPDF) of  $z_i$ ,  $\dot{z}_i$ , and  $y_i$  is [16]

$$p_{\dot{z}_i z_i y_i}(\dot{z}_i, z_i, y_i) = p_{\dot{z}_i}(\dot{z}_i | z_i, y_i) p_{y_i}(y_i) y_i p_{x_i}(z_i y_i). \quad (20)$$

Furthermore, the JPDF of  $z_i$  and  $\dot{z}_i$  is [17]

$$p_{\dot{z}_i z_i}(\dot{z}_i, z_i) = \int_0^{\infty} p_{\dot{z}_i z_i y_i}(\dot{z}_i, z_i, y_i) dy_i. \quad (21)$$

The LCR of the SIR  $z_i$  at the SC receiver output is defined as the mean value of the first derivative. By averaging, LCRs are

$$N_{z_i}(z_i) = \frac{f_m \sqrt{2\pi}}{e^{K_i + (m\lambda^2/\Omega_i)}} \sum_{i_1=0}^{+\infty} \sum_{i_2=0}^{+\infty} \frac{m^{2i_1+m-1/2} K_i^{i_2} \lambda^{2i_1}}{i_1! i_2! \Gamma(i_1+m)} \times \frac{z_i^{2i_1+2m-1} s_i^{i_1+m-1/2} (K_i+1)^{i_2+1/2} \Gamma(i_1+i_2+m+1/2)}{\Gamma(i_2+1)\Omega_i^{i_1-i_2-1/2} ((1+K_i)\Omega_i + ms_i z_i^2)^{i_1+i_2+m}}. \quad (22)$$

The formula for LCR for the output SIR  $z$  is given by ((8) in [18])

$$N_{z|\Omega_i, s_i}(z) = L(F_{z_i}(z_i))^{L-1} N_{z_i}(z_i). \quad (23)$$

If you put equations (10) and (22) in (23), with  $i = \{2, \dots, L\}$ , LCR of the SIR  $z$  at the SC receiver output finally is

$$\begin{aligned}
 N_{z|\Omega_i s_i}(z) = & L \frac{f_m \sqrt{2\pi}}{e^{K_i + (m\lambda^2/\Omega_i)}} \sum_{i_1=0}^{+\infty} \sum_{i_2=0}^{+\infty} \frac{K_i^{i_2}}{i_1! i_2!} \times \\
 & \times \frac{m^{2i_1+m-1/2} \lambda^{2i_1} z^{2i_1+2m-1} s_i^{i_1+m-1/2} (K_i+1)^{i_2+1/2} \Gamma(i_1+i_2+m+1/2)}{\Gamma(i_1+m)\Gamma(i_2+1)\Omega_i^{i_1-i_2-1/2} \left( (1+K_i)\Omega_i + m s_i z_i^2 \right)^{i_1+i_2+m}} \times \\
 & \times \left( e^{-\frac{m}{\Omega_i} \lambda^2} e^{-K_i} \sum_{i_3=0}^{+\infty} \sum_{i_4=0}^{+\infty} \frac{K_i^{i_4} \lambda^{2i_3} \Gamma(i_3+i_4+m+1)}{i_3! i_4! \Gamma(i_3+m)\Gamma(i_4+1)} \left( \frac{m}{\Omega_i} \right)^{i_3} \right. \\
 & \left. \times B \frac{m s_i z_i^2}{\Omega_i (1+K_i) + m s_i z_i^2} (i_3+m, i_4+1) \right)^{L-1}. \quad (24)
 \end{aligned}$$

Based on (24), some graphs will be plotted using Wolfram Mathematica and Origin to highlight the impact of fading and CCI parameters and the diversity combining that was used.

### III. PRESENTATION AND ANALYSIS OF THE CALCULATED SYSTEM PERFORMANCE

To analyse the impact of severity parameters of BX fading and CCI on the concerned performance of LCR normalised by  $f_m$ , we use two plotted graphs versus output SIR, in Figs. 1 and 2. Besides, minimal correlation is assumed between input branches in multi-branch SC receiver.

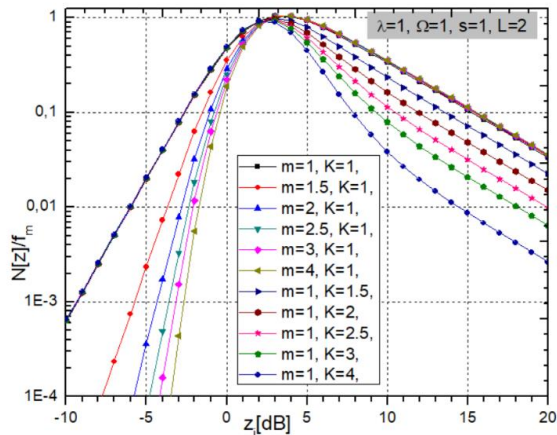


Fig. 1. Normalised LCR of the multi-branch SC receiver versus SIR for different values of the BX fading parameter  $m$  and the Rician factor  $K$ .

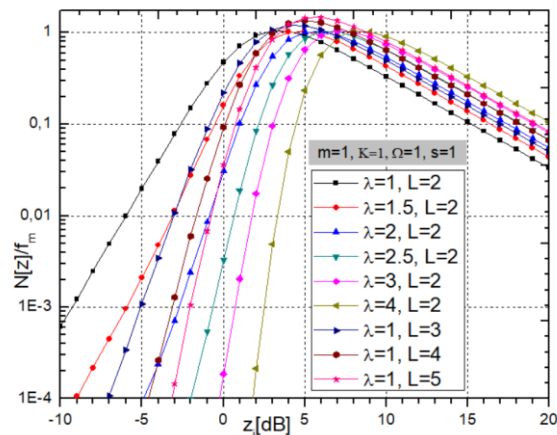


Fig. 2. Normalised LCR of the multi-branch SC receiver versus SIR for different values of the BX fading parameter  $\lambda$  and the number of branches  $L$ . Without loss of generality, we consider BX fading and CCI powers to be equal with the same values:  $\Omega_1 = \Omega_2 = \dots = \Omega_L = \Omega = 1$  and  $s_1 = s_2 = \dots = s_L = s = 1$ .

From the graph in Fig. 1, we can see that for small signal values,  $z < 0$ , and due to the increase of the BX fading parameter  $m$ , the LCR decreases and the system has better characteristics, as the theory says. It is also possible to see from Fig. 1 that LCR decreases for larger, positive values of the SIR  $z$ , when the Rician factor  $K$  increases. This means that the system has better characteristics.

From Fig. 2, one can remark that when the BX fading parameter  $\lambda$  increases, for small SIR values, the LCR decreases. Also, from this figure, it is possible to see that LCR decreases with increasing number of branches  $L$ . These increases of  $\lambda$  and  $L$  improve the system performance.

After drawing these graphs, two Tables, Table I and Table II, are obtained. In them, the number of addends that should be summed in (24) for LCR to reach accuracy at the fifth significant digit is shown. In Table I, the parameters  $m$  and  $K$  are variable, while other parameters have constant values:  $\Omega = 1$ ,  $s = 1$ ,  $\lambda = 1$ ,  $L = 2$ . In Table II, the variables are  $\lambda$  and  $L$ , while other parameters are:  $\Omega = 1$ ,  $s = 1$ ,  $m = 1$ ,  $K = 1$ .

From these tables, it is possible to conclude that when the parameters  $m$  and  $K$  increase, it is necessary to add a larger number of terms in the sum to achieve convergence of the expression. It means that the series converges more slowly. Also, when the parameter  $\lambda$  is increasing, a larger number of elements in the sum are required to be summed, and the series converges more slowly. With increasing number of input branches  $L$ , the number of terms in the sum is not too large, as fast convergence is achieved.

TABLE I. NUMBER OF ADDENDS IN THE SUM IN THE EXPRESSION (24) FOR VARIABLE  $m$  AND  $K$ .

	$z = -10$ dB	$z = 0$ dB	$z = 10$ dB
$m = 1, K = 1$	5	9	8
$m = 1.5, K = 1$	6	8	9
$m = 2, K = 1$	8	9	11
$m = 2.5, K = 1$	9	9	12
$m = 3, K = 1$	9	11	14
$m = 4, K = 1$	10	13	15
$m = 1, K = 1.5$	6	10	9
$m = 1, K = 2$	7	12	10
$m = 1, K = 2.5$	8	12	10
$m = 1, K = 3$	9	14	12
$m = 1, K = 4$	11	16	13

TABLE II. NUMBER OF ADDENDS IN THE SUM IN THE EXPRESSION (24) FOR VARIABLE  $\lambda$  AND  $L$ .

	$z = -10$ dB	$z = 0$ dB	$z = 10$ dB
$\lambda = 1.5, L = 2$	5	8	12
$\lambda = 2, L = 2$	8	9	16
$\lambda = 2.5, L = 2$	8	10	21
$\lambda = 3, L = 2$	9	15	25
$\lambda = 4, L = 2$	9	22	37
$\lambda = 1, L = 3$	8	7	9
$\lambda = 1, L = 4$	8	8	8
$\lambda = 1, L = 5$	9	7	9

Given that the BX fading distribution is a general distribution, for some special parameter values, it is possible to verify the results obtained in this work through the results of our previous papers [19], [20], where the known fading distributions that can be obtained from the BX distribution were analysed.

It can be mentioned that the parameters of the  $\kappa$ - $\mu$  distribution are related to the parameters of the BX distribution as  $\kappa_i = \lambda_i^2/\Omega_i$  and  $\mu_i = m_i$  so that from (24), (20) from [19] can be obtained. Onwards, the Nakagami- $m$

distribution will be obtained from the BX distribution by setting the parameter  $\lambda$  to be equal to 0, as well as from  $\kappa$ - $\mu$  distribution by putting  $\mu = m$  and  $\kappa = 0$ . In this way, (21) of [20] is connected with (24) from this paper, i.e., with (20) of [19].

#### IV. DETERMINATION OF QoS USING CLASSIFICATION IN WEKA

Predictive models that leverage machine learning techniques are among the enablers when it comes to innovative use cases and novel functionalities within state-of-the-art wireless and mobile networks. Notable scenarios include network load prediction, anomaly detection, adaptive QoS adjustment [21]. This paper proposes an approach to determination of QoS level based on supervised machine learning classification methods, taking into account the previously derived LCR value as one of the inputs among the other factors: 1) number of service users within area of interest; 2) identifier of base station responsible for providing service in that area; 3) identifier of area under consideration 4) day of week. However, when it comes to the output of the predictive model, it represents the estimation of the QoS level, which is categorical and could have one of the following values: 0 - presence of anomalies/malfunction, 1 - low, 2 - acceptable, 3 - high. In Table III, a layout of the underlying data set is shown.

Regarding the implementation, we make use of a free framework in Java programming language, Waikato Environment for Knowledge Analysis (Weka) Application Programming Interface (API) [22]. A similar approach has been adopted in our previous work [23], but ABEP was considered instead of LCR and a different type of fading and co-channel interference combination as well. Weka API for Java includes a wide collection of machine learning algorithms, which are free to use and are released under the GNU public licence. It provides functionality covering many aspects related to data access and management, analysis, and visualisation. When it comes to classification methods, Weka supports those that are commonly used, such as the decision table, stump, tree (known as J48), and k-nearest neighbors algorithm (k-NN), referred to as instance based learning (IBk).

Figure 3 illustrates the complete workflow of our approach. In the beginning, the user creates a network model in our simulation and planning environment [24]. Once the model is complete, it is processed for the purpose of LCR calculation based on the general-purpose GPU (GPGPU) method [24], which provides significant speed-up compared to the traditional central processing unit (CPU)-only-based approach. Furthermore, once the LCR values are calculated and other inputs are taken from the network model, a classifier for the determination of the QoS level using Weka is trained.

The training phase contains several sub-steps:

1. Convert CSV data from network planning tool Weka instances suitable for manipulation;
2. Selection of the target variable;
3. Instancing of the classifier model object for a given set of instances [25].

Finally, the model is trained and evaluated. After that, we can use the model to perform predictions on previously

unseen samples. Additionally, based on the results of the predictions, the adaptation of base stations and the underlying carrier infrastructure can be carried out with the aim of keeping the perceived quality of use at a satisfactory level, such as turning off (in case of malfunction and anomalies) or on (compensate for the decrease in QoS).

TABLE III. QoS LEVEL DETERMINATION DATA SET LAYOUT.

LCR	Number of users	Area Id	BS Id	Day of week	QoS
-----	-----------------	---------	-------	-------------	-----

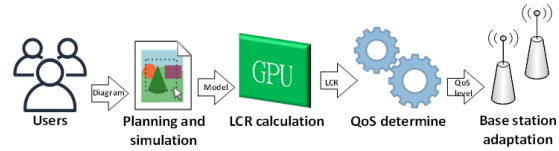


Fig. 3. Machine learning workflow leveraging Weka for QoS estimate.

Furthermore, Table IV gives an overview of the experiments and evaluation of the predictive model, considering both the prediction quality (metric such as accuracy) and the processing time required to train a classifier training. The experiments were executed on a laptop with given characteristics: Intel Core i5-10300H quad-core 2.50 GHz CPU, 8 GB of DDR4 RAM, and 512 GB SSD storage. The data set under consideration consisted of 20,000 entries, divided into training (75 %) and test set (25 %).

TABLE IV. EXPERIMENTS AND EVALUATION RESULTS.

Algorithm	Training [s]	Accuracy [%]
DecisionTable	16.8	93.5
J48	5.9	89.2
DecisionStump	4.	84.1
IBk	7.1	87.2

Taking into account the results obtained, it can be noticed that the DecisionTable algorithm shows the best prediction quality in terms of accuracy, while the training time is the longest. On the other hand, considering the rest of evaluated algorithms, we have the following situation:

1. J48 is one place behind, but with a much shorter training time;
2. Despite the fact that DecisionStump had the shortest processing time, it had the lowest accuracy, while k-NN IBk shows slightly better results, but is slower in general.

#### V. CONCLUSIONS

In this work, a wireless system impacted by Beaulieu-Xie fading and Rician co-channel interference has been analysed. The BX fading distribution is a very important newly performed distribution because it describes wireless channels very well and has the property of generality due to its distribution parameters connected to the parameters of well-known distributions. An SC diversity receiver was used to alleviate multi-path BX fading and CCI effects. Such a scenario was not considered in earlier works with BX fading. An expression for LCR was derived for such a receiver. Based on this expression and plotted graphs for LCR of the described scenario, the parameters influence and

quantity of improvement achieved with diversity combiner have been highlighted. The results obtained can be validated by reducing the expression to special cases of known fading channels previously considered in our previous papers. Additionally, we have proposed the software environment for LCR simulation for the observed system under the influence of BX fading and Rician CCI, leveraging the calculated LCR value as one of the inputs for a classification-based method aiming at QoS estimation. Based on the results achieved, our approach shows promising accuracy and training execution time.

In the future, we plan to work on adaptability mechanisms that would dynamically adjust the underlying infrastructure (turn on additional modules or turn off the faulty one) based on the current QoS level outcome. Also, in the next work, the influence of other distributions of fading and CCI, as well as their combinations, will be analysed. Likewise, the use of other diversity combining schemes, as is the optimal maximum ratio combining model, will be taken into consideration.

#### ACKNOWLEDGMENT

This paper is made as a cooperation in the frame of the bilateral project “Development of Secure and Spectral Efficient Simultaneous Wireless Information and Power Transfer Systems for Large-Scale Wireless Networks” between the Republics of Serbia and India, under the cover of the Ministry of Science, Technological Development and Innovation of the Republic of Serbia.

#### CONFLICTS OF INTEREST

The authors declare that they have no conflict of interest.

#### REFERENCES

- [1] M. K. Simon and M.-S. Alouini, *Digital Communication over Fading Channels*, 2nd ed. Wiley-IEEE Press, 2005. DOI: 10.1002/0471715220.
- [2] T. S. Rappaport, G. R. MacCartney, M. K. Samimi, and S. Sun, “Wideband millimeter-wave propagation measurements and channel models for future wireless communication system design”, *IEEE Transactions on Communications*, vol. 63, no. 9, pp. 3029–3056, 2015. DOI: 10.1109/TCOMM.2015.2434384.
- [3] M. K. Samimi, G. R. MacCartney, S. Sun, and T. S. Rappaport, “28 GHz millimeter-wave ultrawideband small-scale fading models in wireless channels”, in *Proc. of 2016 IEEE 83rd Vehicular Technology Conference (VTC Spring)*, 2016, pp. 1–6. DOI: 10.1109/VTCSpring.2016.7503970.
- [4] J. M. Romero-Jerez, F. J. Lopez-Martinez, J. F. Paris, and A. J. Goldsmith, “The fluctuating two-ray fading model: Statistical characterization and performance analysis”, *IEEE Transactions on Wireless Communications*, vol. 16, no. 7, pp. 4420–4432, 2017. DOI: 10.1109/TWC.2017.2698445.
- [5] A. Olutayo, “A novel fading model for emerging wireless communication systems”, Ph.D. dissertation, The University of British Columbia, Okanagan, 2021.
- [6] N. C. Beaulieu and X. Jiandong, “A novel fading model for channels with multiple dominant specular components”, *IEEE Wireless Communications Letters*, vol. 4, no. 1, pp. 54–57, 2015. DOI: 10.1109/LWC.2014.2367501.
- [7] V. Kansal and S. Singh, “Analysis of effective capacity over Beaulieu-Xie fading model”, in *Proc. of 2017 IEEE International WIE Conference on Electrical and Computer Engineering (WIECON-ECE)*, 2017, pp. 207–210. DOI: 10.1109/WIECON-ECE.2017.8468917.
- [8] V. Kansal and S. Singh, “Error performance of generalized M-ary QAM over the Beaulieu-Xie fading”, *Telecommunication Systems*, vol. 78, pp. 163–168, 2021. DOI: 10.1007/s11235-021-00775-0.
- [9] H. Thien Van, “Threshold-based Wireless-based NOMA Systems over Log-Normal Channels: Ergodic Outage Probability of Joint Time Allocation and Power Splitting Schemes”, *Elektronika i Elektrotehnika*, vol. 27, no. 3, pp. 78–83, Jun. 2021. DOI: 10.5755/j02.eie.28971.
- [10] M. Kaur and R. K. Yadav, “Performance analysis of Beaulieu-Xie fading channel with MRC diversity reception”, *Transactions on Emerging Telecommunications Technologies*, vol. 31, no. 7, p. e3949, 2020. DOI: 10.1002/ett.3949.
- [11] S. O. Rice, “Statistical properties of a sine wave plus random noise”, *The Bell System Technical Journal*, vol. 27, no. 1, pp. 109–157, 1948. DOI: 10.1002/j.1538-7305.1948.tb01334.x.
- [12] M. Patzold, W. Dahech, and N. Youssef, “Level-crossing rate and average duration of fades of non-stationary multipath fading channels”, in *Proc. of 2017 IEEE 28th Annual International Symposium on Personal, Indoor, and Mobile Radio Communications (PIMRC)*, 2017, pp. 1–7. DOI: 10.1109/PIMRC.2017.8292439.
- [13] I. S. Gradshteyn and I. M. Ryzhik, *Table of Integrals, Series, and Products*. Academic Press, Cambridge, MA, USA, 2007.
- [14] W. Wongtrairat and P. Supnithi, “New simple form for PDF and MGF of Rician fading distribution”, in *Proc. of 2011 International Symposium on Intelligent Signal Processing and Communications Systems (ISPACS)*, 2011, pp. 1–4. DOI: 10.1109/ISPACS.2011.6146087.
- [15] A. Jeffrey and H. H. Dai, *Handbook of Mathematical Formulas and Integrals*, 4th ed. Academic Press, 2008.
- [16] S. Suljović, D. Krstić, D. Bandjur, S. Veljković, and M. Stefanović, “Level crossing rate of macro-diversity system in the presence of fading and co-channel interference”, *Revue Roumaine des Sciences Techniques*, vol. 64, no. 1, pp. 63–68, 2019.
- [17] D. Krstić, S. Suljović, D. Milić, S. Panić, and M. Stefanović, “Outage probability of macro-diversity reception in the presence of Gamma long-term fading, Rayleigh short-term fading and Rician co-channel interference”, *Annals of Telecommunications*, vol. 73, pp. 329–339, 2018. DOI: 10.1007/s12243-017-0593-4.
- [18] C. Stefanovic, S. Veljković, M. Stefanović, S. Panić, and S. Jovković, “Second order statistics of SIR based macro diversity system for V2I communications over Composite fading channels”, in *Proc. of 2018 First International Confer. on Secure Cyber Comp. and Communication (ICSCCC)*, 2018, pp. 569–573. DOI: 10.1109/ICSCCC.2018.8703293.
- [19] D. Krstic, S. Suljovic, N. Petrovic, Z. Popovic, and M. Stefanovic, “Level crossing rate of next generation wireless systems with selection combining in the presence of k- $\mu$  fading and interference: Derivation and simulation”, in *Proc. of 2021 16th International Conference on Telecommunications (ConTEL)*, 2021, pp. 4–9. DOI: 10.23919/ConTEL52528.2021.9495974.
- [20] S. Vasic, D. Rančić, D. Milić, N. Petrović, R. Stefanović, and S. Suljović, “Performance simulation for LCR of 5G wireless system with L-branch SC receiver in k- $\mu$  fading and Nakagami- $m$  interference channel”, in *Proc. of 2021 20th International Symposium INFOTEH-JAHORINA (INFOTECH)*, 2021, pp. 1–6. DOI: 10.1109/INFOTEH51037.2021.9400681.
- [21] D. Krstić, N. Petrović, and I. Al-Azzoni, “Model-driven approach to fading-aware wireless network planning leveraging multiobjective optimization and deep learning”, *Mathematical Problems in Engineering*, vol. 2022, art. ID 4140522, 2022. DOI: 10.1155/2022/4140522.
- [22] Weka 3: Machine Learning Software in Java. [Online]. Available: <https://www.cs.waikato.ac.nz/ml/weka/>
- [23] D. Krstic, S. Suljovic, N. Petrovic, Z. Popovic, and S. Minic, “MGF based calculation and simulation of ABEP for multi-branch SC receiver in an environment under  $\alpha$ - $\kappa$ - $\mu$  fading and co-channel interference”, in *Proc. of 2022 International Balkan Conference on Communications and Networking (BalkanCom)*, 2022, pp. 26–30. DOI: 10.1109/BalkanCom55633.2022.9900869.
- [24] N. Petrović, S. Vasić, D. Milić, S. Suljović, and S. Koničanin, “GPU-supported simulation for ABEP and QoS analysis of a combined macro diversity system in a Gamma-shadowed k- $\mu$  fading channel”, *Facta Universitatis, Series: Electronics and Energetics*, vol. 34, no. 1, pp. 89–104, 2021. DOI: 10.2298/FUEE2101089P.
- [25] N. Petrović, “Machine learning within information systems course using Weka in Java: Monkeypox case studies”, in *Proc. of XVI International SAUM Conference*, 2022, pp. 115–118. DOI: 10.13140/RG.2.2.26822.75842.



This article is an open access article distributed under the terms and conditions of the Creative Commons Attribution 4.0 (CC BY 4.0) license (<http://creativecommons.org/licenses/by/4.0/>).